Tunneling spectroscopy of two-dimensional surface states in gapless p-HgCdTe

G. M. Min'kov, O. É. Rut, V. A. Larionova, and A. V. Germanenko

Institute of Physics and Applied Mathematics, Ural University, 620083 Ekaterinburg, Russia
(Submitted 14 October 1993)
Zh. Eksp. Teor. Fiz. **105**, 719–738 (March 1994)

Tunneling spectroscopy in a magnetic field has been used for the first time to experimentally investigate the spectrum of size-quantized electron states in a surface quantum well in gapless *p*-HgCdTe semiconductors. It has been shown that spin splitting of the tunneling conductivity oscillations is not observed upon tunneling into two-dimensional electron states and that the dependence of their effective mass on the quasimomentum parallel to the surface is not described in the simple "quasiclassical" model. The spectrum of size-quantized states in a semiconductor described by the Kane Hamiltonian in a surface quantum well with a model rectangular potential has been calculated to qualitatively interpret the experimental results. It has been shown that the main features of the calculated spectrum, viz., the existence of a single nonspin-degenerate localized state when the potential well is shallow and the closeness of the effective mass of two-dimensional electrons to the effective mass of electrons in the bulk of the semiconductor, fit the experimental results.

1. INTRODUCTION

Systems with a two-dimensional (2D) electron gas in both broadband and narrow-gap semiconductors with a positive gap have been earnestly investigated during the last 10–15 years. Experimental investigations of the dispersion law, effective mass, and g factor have been performed on structures of various types: surface quantum wells and quantum wells based on heterostructures and δ-doped layers.[1] In most studies the energy spectrum was theoretically described in a quasiclassical approximation, which provides good agreement with experiment (see Refs. 2–5 and the references therein).

Two-dimensional electron states in the surfaces quantum wells of gapless semiconductors have been investigated to a considerably lesser extent. This is due primarily to the fact that the traditional experimental methods are virtually inapplicable to the investigation of such systems. For example, it is in fact impossible to extract information about 2D states from galvanomagnetic measurements due to the strong shunting effect of the bulk of a semiconductor. The high optical density of the bulk of a semiconductor renders investigations of the absorption and magnetoabsorption of light useless.

Experimental results have been obtained only with the aid of the voltage-capacitance spectroscopy of metal–insulator–semiconductor (MIS) structures in a quantizing magnetic field.[4,5] Just as in the case of narrow–gap semiconductors, Radantsev *et al.* were able to explain all of their observations (the subband starting voltages, the effective masses, etc.) in the framework of a simple quasiclassical approximation. This in itself is surprising, since the conduction band in these gapless semiconductors is the quadruply degenerate Γ_8 band, rather than the doubly degenerate Γ_6 band, as in semiconductors with an open forbidden gap. This circumstance may be significant in shaping the energy spectrum of a spatially restricted semiconductor. Thus, it was predicted in Refs. 6–8 that an additional branch of 2D electron states, which does not exist in the quasiclassical treatment and which might be manifested experimentally, should exist on a gapless-semiconductor-insulator boundary even in the absence of an attractive surface potential.

This communication presents the results of investigations of the spectrum of 2D states in the surface quantum well of a gapless HgCdTe semiconductor obtained by tunneling spectroscopy. This method is based on studying the features of the current-voltage characteristics of tunnel structures. In principle, the dependence of the tunneling current on the applied voltage $j(V)$ in MIS structures contains information about the energy spectrum of the current carriers in both electrodes and in the insulator. However, the most dependable and reliable information about the energy spectrum of the current carriers in a semiconductor can be obtained by investigating plots of $j(V)$ and determining $\sigma=dj/dV$ in a magnetic field, since the distance between the Landau levels in the semiconductor can be determined directly as a function of the magnetic field over a broad range of energies in this case.[9,10]

The first detailed investigations of tunneling conductivity oscillations in a magnetic field were performed in Ref. 9 on *n*-InAs-oxide-Pb structures. There is always considerable warping of the bands on the surface of *n*-InAs with the resultant formation of size-quantized electron states. It was shown that superposition of the tunneling conductivity oscillations associated with quantization of the spectra of the bulk and 2D states is observed in a magnetic field normal to the surface of a tunnel junction ($\mathbf{H}\parallel\mathbf{n}$, where $\mathbf{n}$ is a normal to the plane of the junction). When $\mathbf{H}\perp\mathbf{n}$, 2D states are not quantized by the magnetic field, and the tunneling conductivity oscillations are asso-

 © 1994 American Institute of Physics

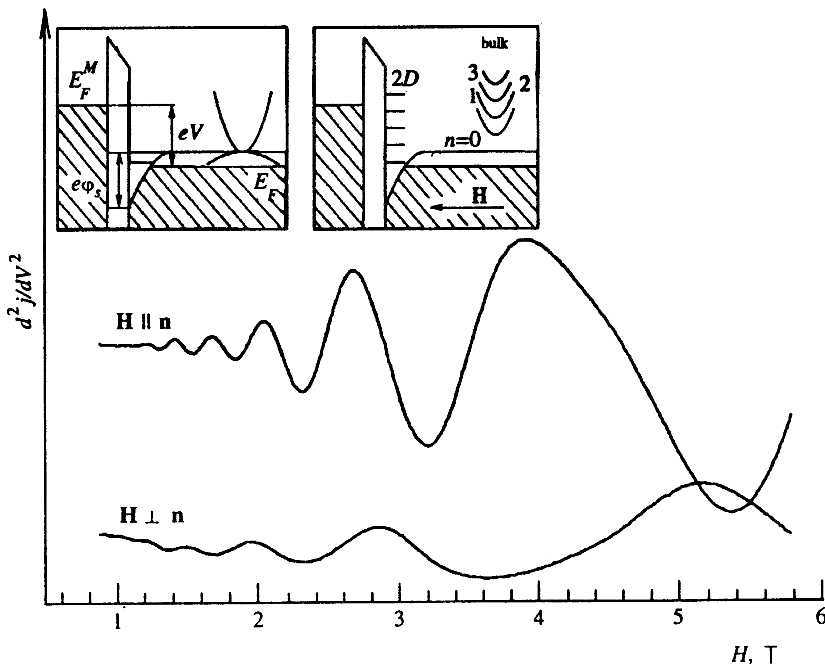

FIG. 1. Dependence of d^2j/dV^2 on H at $V=80$ mV in two orientations of the magnetic field for a tunnel junction prepared on p-HgCdTe with $E_g=-60$ meV and $N_a-N_d=6\cdot10^{18}$ cm^{-3} at $T=4.2$ K. Energy diagrams of a tunnel junction in the absence of a magnetic field (on the left) and in a magnetic field perpendicular to the surface of the semiconductor is presented in the inserts.

ciated only with quantization of the spectrum of the carriers in the bulk of the semiconductor. Experimental investigations of the spectrum of the bulk carriers in gapless HgTe, HgCdTe,[10] HgMnTe,[11] and HgSe[12] semiconductors have also been performed by tunneling spectroscopy.

The results of the experimental investigations of spectrum of 2D electrons in gapless p-HgCdTe semiconductors by tunneling spectroscopy in a quantizing magnetic field will be presented in Sec. 2. In Sec. 3 they will be compared with the results of the usually employed "quasiclassical" approximation. A calculation of the spectrum of 2D electrons in the surface quantum well in gapless semiconductor in the framework of the two-band Kane model, which accurately takes into account the interaction of the closely situated Γ_8 and Γ_6 bands, will be presented in Sec. 4. The results of this calculation will be compared with experiment in Sec. 5.

2. EXPERIMENTAL RESULTS

The differential conductivity and its derivative with respect to the voltage were investigated as a function of the magnetic field and the voltage on a p-$Hg_{1-x}Cd_xTe$-insulator-metal structure in magnetic fields up to 6 T at $T=2$–40 K. Tunnel junctions were prepared on highly doped samples of p-$Hg_{1-x}Cd_xTe$ ($0.08<x<0.14$) with a concentration of uncompensated acceptors $N_a-N_d=(1$–$6)\cdot10^{18}$ cm^{-3}. After mechanical grinding and polishing, the samples were etched in a 10% solution of bromine in butanol and then washed in butanol. Two or three layers of a Langmuir–Blodgett film of heptylcyanoacrylic acid (C_7-CAA) were transferred to the freshly etched surface as a tunneling-transparent barrier. The method for transferring monolayers to the surface of a sample was described in Ref. 13. Then a metallic bilayer electrode (Al+Pb) was spray-deposited through a mask.

Typical plots of the dependence of d^2j/dV^2 on the magnetic field in the $\mathbf{H}\perp\mathbf{n}$ and $\mathbf{H}\parallel\mathbf{n}$ orientations are presented in Fig. 1. As we have already noted, the tunneling conductivity oscillations observed for $\mathbf{H}\perp\mathbf{n}$ are associated only with quantization of the spectrum of bulk carriers. At a fixed bias they are periodic with respect to the reciprocal of the magnetic field, and the period is identical on all tunnel structures prepared on the same sample.

The situation is more diverse in the $\mathbf{H}\parallel\mathbf{n}$ orientation. Three cases were observed for the tunnel junctions investigated (even for junctions prepared on the same sample): 1) the amplitudes of the oscillations A and their periods with respect to the reciprocal of the magnetic field $\Delta(1/H)$ for $\mathbf{H}\parallel\mathbf{n}$ and $\mathbf{H}\perp\mathbf{n}$ differ, i.e., $\Delta_\parallel(1/H)<(\Delta_\perp(1/H)$, and $A_\parallel>A_\perp$ (as in Fig. 1); 2) the periods of the oscillations are nearly identical within the range of accuracy, but the amplitudes differ significantly, i.e., $A_\parallel>A_\perp$; 3) the periods of the oscillations are equal and the amplitudes are close.

The investigations show that these three cases can be distinguished by the different values of the surface potential attracting the electrons. In the first case it is so great that size-quantized states form in it. In the third case there is no attracting potential, and tunneling into bulk states occurs in both orientations of the magnetic field. (We examined this case and the special features of the tunneling of electrons into different spin states in Ref. 14.) In the second case, as will be shown below, the tunneling current oscillations are coupled when $\mathbf{H}\parallel\mathbf{n}$, despite the closeness of the periods, just as in the first case with tunneling into 2D states.

We shall first examine the experimental results corre-

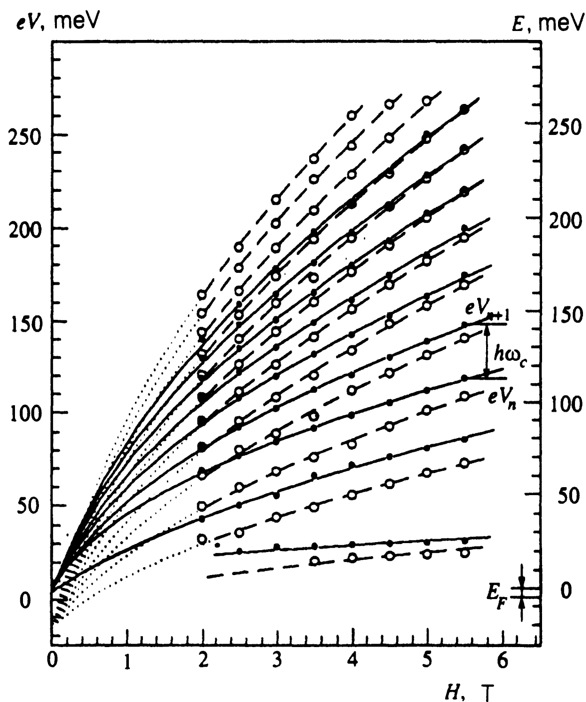

FIG. 2. Position of the maxima of the tunneling conductivity oscillations for a junction from the first group (the same tunnel junction as in Fig. 1) in two orientations of the magnetic field: **H**⊥ **n** (●), **H**∥ **n** (○).

sponding to the first case. Plotting the positions of the oscillations in V versus H coordinates, we obtain a network of levels that reflects the displacement of the Landau levels in a magnetic field. The dependence for one of the samples investigated in both orientations of the magnetic field is presented in Fig. 2. It is seen that behavior of the oscillations for **H**⊥ **n** and **H**∥ **n** differs, and if their positions are extrapolated to $H=0$, they converge to different values of eV.

According to the discussion in Refs. 9 and 10, when **H**⊥ **n**, tunneling conductivity oscillations are caused by tunneling into states of bulk Landau levels of the semiconductor with energies $E=E_F+eV$ (E_F is the Fermi energy of the semiconductor). Therefore, at a fixed bias the oscillations are periodic with respect to the inverse magnetic field, and in an isotropic semiconductor their period is determined by the value of the quasimomentum (k) of the bulk carriers at the energy $E=E_F+eV$ (see the inserts in Fig. 1):

$$\Delta(1/H)\,|_V=(2e)/(c\hbar k^2|_{E_F+eV}). \qquad (1)$$

Thus, the dispersion law of the electrons in the semiconductor can be reconstructed by measuring the period of the oscillations with respect to the reciprocal of the magnetic field at different applied voltages. The plot of $E(k)$ obtained from such measurements (Fig. 3) is described well in the Kane model with the parameters $P=8.2\cdot 10^{-8}$ eV·cm, $E_g=-60$ meV, and $\Delta\equiv E(\Gamma_8)-E(\Gamma_7=1$ eV (the details of the analysis of oscillations in this orientation of the magnetic field were presented in Refs. 10 and 12).

In the **H**∥ **n** orientation the tunneling conductivity oscillations have a significantly higher amplitude than in the **H**⊥ **n** orientation (by a factor of 2–10 for different tunneling constants, depending on the bias voltage and the magnetic field strength), and are caused by tunneling into Landau levels of two-dimensional states localized at the surface. This follows from the typical angular dependence (Fig. 4) of the position of the oscillations:

$$H^i(\theta)=H^i_{\parallel}\,/\cos\theta$$

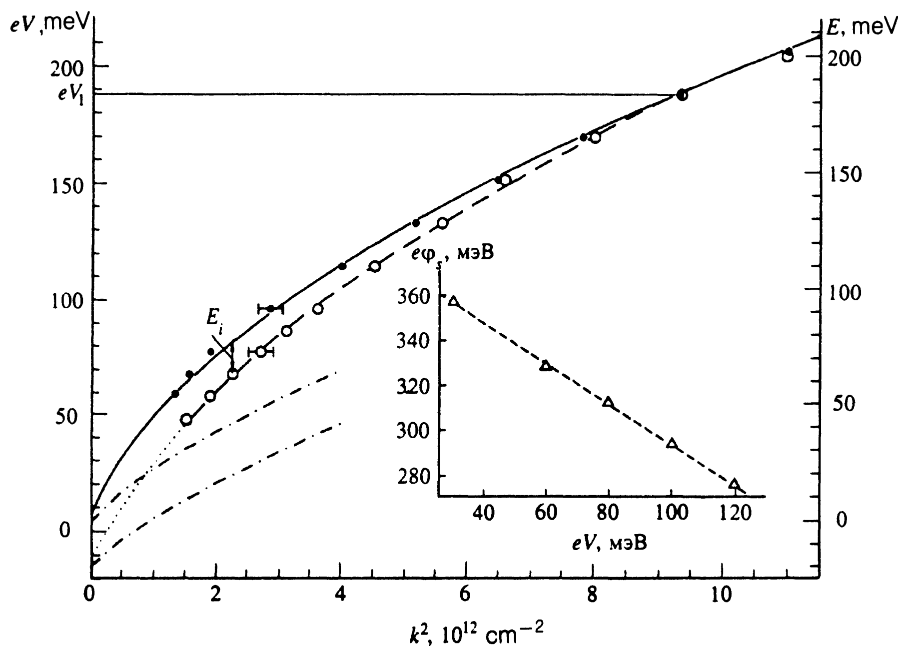

FIG. 3. Dependence of k^2 on the voltage applied to the same tunnel junction as in Fig. 2: **H**⊥ **n** (●), **H**∥ **n** (○). The solid curve is the dispersion law calculated in the Kane model, the dashed line was constructed from experimental points, and the dash-dot lines are the dispersion laws of the 2D electrons calculated in the "quasiclassical" model at fixed values of $e\varphi_s$: 380 meV (lower curve) and 340 meV (upper curve). The dependence of the surface potential on the applied voltage calculated in the "quasiclassical" model is shown in the insert.

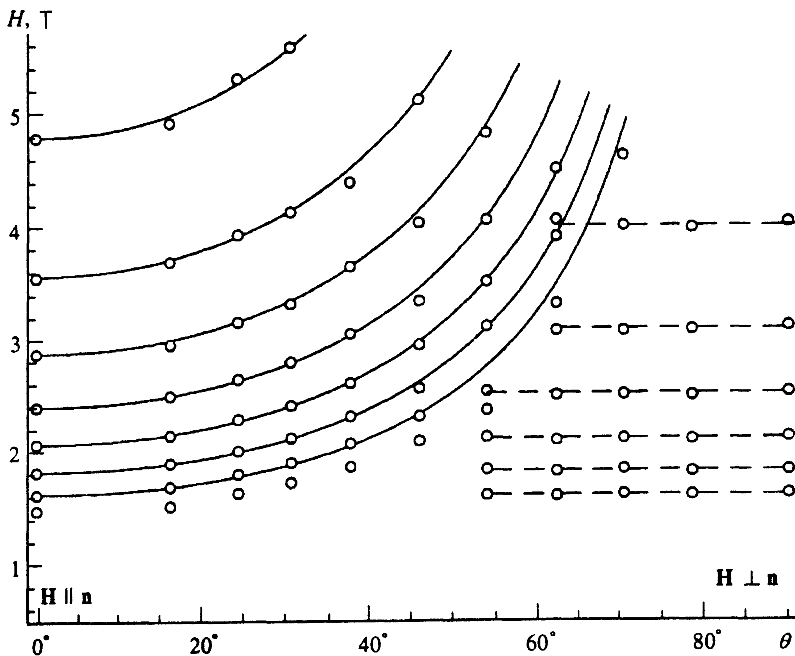

FIG. 4. Angular dependence of the position of the tunneling conductivity maxima at $V=120$ mV for the same junction as in Figs. 2 and 3.

(H^i is the position of the ith tunneling conductivity extremum, and θ is the angle between **H** and **n**). Such a dependence is observed at $\theta<60°$, since the amplitude of the oscillations associated with tunneling into 2D states decreases with increasing θ, and only the oscillations caused by tunneling into bulk states are observed at $\theta>60°$.

When **H**∥ **n**, the oscillations are also periodic with respect to the reciprocal of the magnetic field, and at applied voltages smaller than a certain value V_1 (Fig. 3) the period of the tunneling conductivity oscillations is smaller in the **H**∥ **n** orientation than in the **H**⊥ **n** orientation. At $V>V_1$ the amplitudes of the oscillations in the two orientations of the magnetic field become similar, and the periods with respect to the reciprocal of the magnetic field are equal to within the experimental errors. When V is increased further, the angular dependence of the position of the oscillations vanishes.

Unexpected results were obtained on the tunnel junctions from the second group, in which the periods of the oscillations with respect to the reciprocal of the magnetic field are equal to within the experimental errors over the entire range of applied voltages, while their amplitudes differ significantly, i.e., $A_{\parallel}>A_{\perp}$ (the sample in Fig. 5). The equality of the periods of the oscillations indicates that the quasimomentum of the states determining the oscillations of the tunneling current are identical; therefore, it would appear that the oscillations in both orientations of the magnetic field are caused by tunneling into Landau levels of bulk states. However, these tunnel junctions exhibit the typical angular dependence of the position of the oscillations $H^i(\theta)=H^i_{\parallel}/\cos\theta$ near **H**∥ **n**, but they display dips in the oscillations in intermediate orientations, which are manifested by a drastic decrease in their amplitude to the point of essentially complete disappearance over a certain range of magnetic field strengths (Fig. 5, $\theta\approx40°$, $H\approx1.5$–2 T). Such behavior of the oscillations is indisputable evidence that they are the result of the superposition of oscillations of two types, one of which has an angular dependence, i.e., is associated with tunneling into 2D states.

Another distinctive feature of the tunneling conductivity oscillations in the samples from the first and second groups, in which they are associated with tunneling into 2D states when **H**∥ **n**, is the lack of spin splitting of the oscillation maxima (Figs. 1 and 5).[1)] This differs radically from the results obtained on samples from the third group, in which the tunneling conductivity oscillations are associated with tunneling into bulk states in all orientations of the magnetic field. In these junctions spin splitting is observed when **H**∥ **n**, and the amplitude of the high-field component decreases monotonically as the field is rotated to **H**⊥ **n** (Fig. 6). As was shown in Ref. 14, the lack of spin splitting of the maxima when **H**⊥ **n** is due to the significantly smaller probability of tunneling into one of the "spin" states (the states of the a series).

The lack of spin splitting upon tunneling into two-dimensional states may be attributed to several factors: 2D states localized at the boundary of a gapless semiconductor are not "spin-degenerate" ("one-spin" states);[2)] the magnitude of the spin splitting is small in comparison to the smearing of the levels; the probabilities of tunneling into different "spin" states differ significantly. Which of these factors is decisive will become clear from a subsequent discussion (Sec. 5). Thus, the tunnel junctions from the first and second groups investigated have 2D electron states in the gapless semiconductor at the boundary with the insulator, and the tunneling into them is responsible for the tunneling conductivity oscillations when **H**∥ **n**. One special feature of the tunneling into these states is the lack of spin splitting of the oscillations.

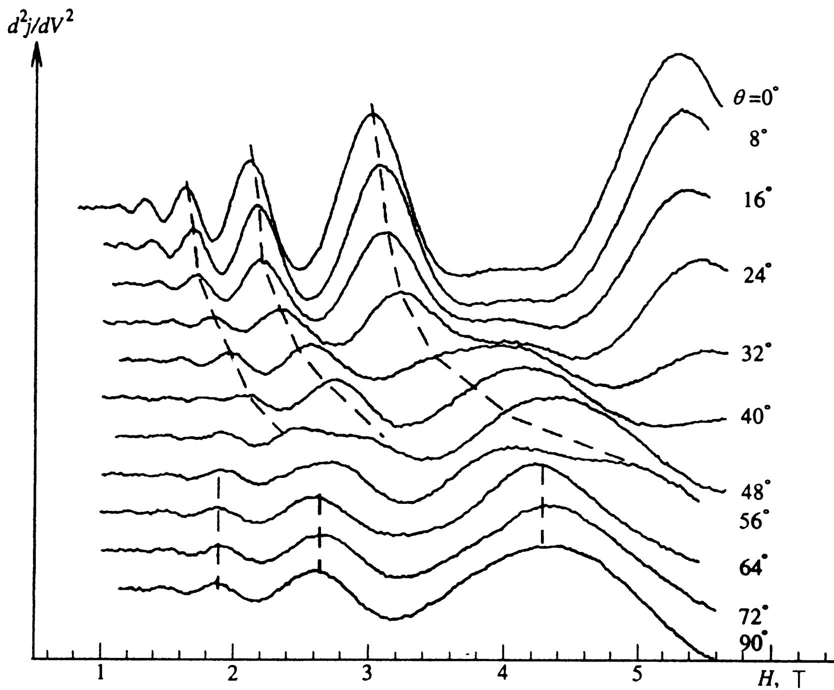

FIG. 5. Oscillations of d^2j/dV^2 at $V=80$ mV and various angles between **H** and **n** for a junction from the second group, in which the periods of the oscillations with respect to the reciprocal of the magnetic field for **H**⊥ **n** and **H**|| **n** are nearly equal. The junction was prepared on p-HgCdTe with $E_g=-60$ meV an $N_a-N_d=6\cdot 10^{18}$ cm^{-3}. $T=4.2$ K. The numbers on the curves are angles in degrees.

3. ANALYSIS OF THE RESULTS IN THE FRAMEWORK OF THE "QUASICLASSICAL" MODEL

Let us analyze our experimental results in the framework of the familiar "quasiclassical" model, which is used to analyze the energy spectrum of 2D states in gapless semiconductors with a largely nonparabolic dispersion law.[15,16] We take a coordinate system with x axis perpendicular to the boundary of the semiconductor and y axis parallel to the two-dimensional wave vector in the plane of the surface. It is assumed in the quasiclassical description that if the dispersion law of the carriers in the bulk of the semiconductor $k^2=f(E)$ is known (we shall consider an isotropic dispersion law) and if we separate the motions along and across the surface, i.e., if we write

$$k^2=k_x^2+k_y^2=f(E),$$

we can find the dispersion law of the 2D states $E(k_y)$ from the quasiclassical quantization condition

$$\int_0^{x_0}\hbar k_x dx=\int_0^{x_0}\sqrt{(f(E)-k_y^2)}dx=\pi(n+\delta),$$

$$n=0,\ 1,\ 2...,\qquad (2)$$

where x_0 and 0 are the classical turning points, $\delta=1$ for an infinite square well, and $\delta=3/4$ for a surface quantum well.

Let us analyze the experimental results obtained in the context of this model. In gapless HgCdTe the dispersion law has the form

$$k^2=\frac{E(E-E_g)(E+\Delta)}{P^2(E+2\Delta/3)}.\qquad (3)$$

The variation of the potential at the surface is given by the solution of the Poisson equation

$$\nabla_x^2\varphi(x)=\frac{\rho}{\kappa_0\kappa},\qquad (4)$$

where ρ is the charge density and κ is the dielectric constant. At low temperatures in a highly doped p-typed semi-

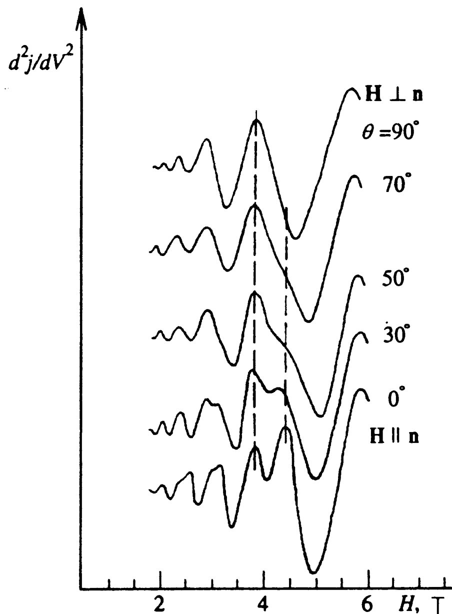

FIG. 6. Oscillations of d^2j/dV^2 at $V=110$ mV and various angles between **H** and **n** for a junction from the third group, in which the oscillations are caused by tunneling into Landau levels of bulk states when **H**⊥ **n** and **H**|| **n**. The junction was prepared on p-HgCdTe with $E_g=-20$ meV and $N_a-N_d=4\times 10^{18}$ cm^{-3}. $T=4.2$ K.

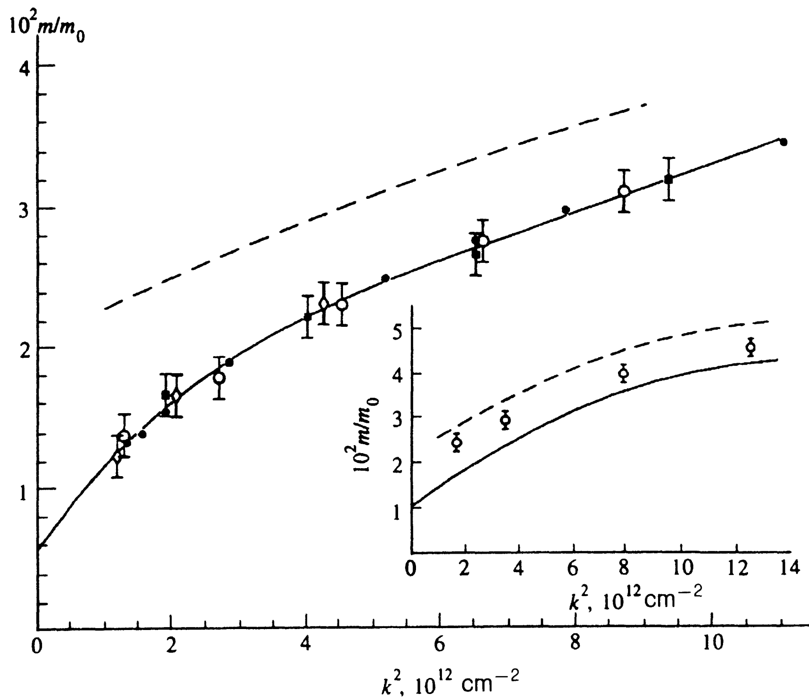

FIG. 7. Dependence of the effective mass of electrons of k^2: ●, ■—for bulk states obtained from the network of levels (Fig. 2) and the temperature dependence of the oscillation amplitude, respectively; ○—for 2D states in the same tunnel junction as in Figs. 2–4; ◇—for 2D states in a tunnel junction from the second group; solid curves—calculation for bulk states in the Kane model; dashed curves—quasiclassical calculation for 2D states. The concentration of uncompensated acceptors in the sample was $6 \cdot 10^{18}$ cm^{-3}. Insert: points—experimental results for a sample with $E_g = -100$ meV and $N_a - N_d = 1.4 \cdot 10^{18}$ cm^{-3}, which were kindly supplied by Radantsev *et al.*;[4,5] solid curve—effective mass for bulk states; dashed curve—quasiclassical calculation for 2D states.

conductor with a low concentration of 2D electrons $[n_s \ll (N_a - N_d)^{2/3}]$, $\rho = e(N_a - N_d)$, and solution (4) has the form

$$\varphi(x) = \varphi_s(1 - x/L)^2, \quad L^2 = \frac{2\varkappa\varkappa_0\varphi_s}{e(N_a - N_d)}, \qquad \varphi_s = \varphi(0). \tag{5}$$

Plugging (3) into (2) and taking into account that in (3) E should be replaced by $E + e\varphi(x)$ in the space-charge region, we obtain an equation whose solution gives the dispersion law $E(k_y)$ of 2D electrons at a fixed value of φ_s. A plot of $E(k_y)$ calculated in this manner for 2D electrons in one of the samples at several values of φ_s is presented in Fig. 3. The strong deviation of the calculated dispersion law of the 2D electrons from experiment should not be considered surprising, since the experimental plot of $eV(k_y)$ in the $\mathbf{H} \parallel \mathbf{n}$ orientation is actually not the dispersion law of the 2D carriers. This is due to the fact that the voltage applied to a tunnel junction alters not only the distance between the Fermi levels of the metal and the semiconductor and thus the energies of the states of the semiconductor, which determine the differential conductivity (see the inserts in Fig. 1), but also the surface potential φ_s. Of course, we can use φ_s as a fitting parameter to describe the experimental dependence of $eV(k_y)$ (Fig. 3). This provides a nearly linear dependence of φ_s on eV (see the insert in Fig. 3). As we see, the condition $\Delta\varphi_s \approx V$ must be satisfied to describe the experimental results in the context of the model under consideration, i.e., practically all of the applied voltage must fall in the space-charge region in the semiconductor, rather than on the barrier. This seems unlikely, since the total resistance of the tunnel junctions investigated (the resistance of the barrier and the resistance of the semiconductor connected in series) was 10–1000 Ω (for different junctions), and it is difficult to imagine that the resistance of the space-charge region in a highly doped p-type gapless semiconductor has such a high value.

Another parameter of the energy spectrum that can be measured by tunneling spectroscopy and can be calculated in the context of the quasiclassical model is the effective mass and its dependence on the quasimomentum.

The cyclotron mass for bulk carriers (m_e) can be determined experimentally both from the network describing the positions of the oscillation maxima in eV versus H coordinates (Fig. 2) and from the temperature dependence of the amplitude of the oscillations,[9,17] which give identical values to within the errors. The cyclotron mass for 2D states (m_s) cannot be determined from the network, since the applied voltage alters the surface potential φ_s and, therefore,

$$eV_{n+1} - eV_n = E_{n+1}(\varphi_s) - E_n(\varphi_s') \neq \hbar \frac{eH}{m_s c}.$$

However, it can be determined, as in the other case, from the temperature dependence of the amplitude of the oscillations. As can be seen from Fig. 7, the experimental values of the cyclotron mass for 2D states is significantly smaller than the theoretical value at all values of the quasimomentum, but they coincide to within the accuracy of the measurements with the effective mass for bulk states. At first glance these results contradict all the preceding findings, from which it was concluded that the quasiclassical ap-

proximation describes all the experimental data.[4,5,18] However, it should be recalled that all the investigations were performed either on lightly doped samples or at high concentrations of electrons (i.e., at large values of k_y), while the calculations show that the difference between the masses of bulk and two-dimensional carriers is greatest when k_y is small and the doping level is high. In addition, in those studies the experimental values of m_s and its dependence on the concentration of 2D carriers n_s (i.e., on k_y^2, since $n_s=k_y^2/2\pi$) where compared with the calculated values and dependence, but not with the bulk-carrier effective mass m_e at the same value of the quasimomentum. Such a comparison (see the insert in Fig. 7) reveals that the experimental values of m_s are close not only to the calculated values of m_s, but also to m_e. Thus, experiments performed either on lightly doped samples or at large values of k_y do not, in fact, make it possible to verify one of the main consequences of quasiclassical calculations of the spectrum of size-quantized states in a nonparabolic gapless semiconductor, viz., that the effective mass of 2D electrons should be greater than the effective mass for bulk states with the same value of the quasimomentum.

In our opinion, the disparity between the results of the simple theoretical model described above and experiment is attributable primarily to the need to correctly take into account the structure of the Hamiltonian and the multicomponent wave function of electrons in a gapless semiconductor. Such calculations of the spectrum of 2D carriers in symmetric heterostructures consisting of a gapless semiconductor and a semiconductor with $E_g>0$ and HgTe–CdTe superlattices have been performed in many studies (see, for example, Refs. 7, 19, 20). We do not know of any calculations of the spectrum in the surface quantum well in gapless semiconductor. The uniqueness of such a structure becomes clear already from the results of Ref. 6, in which the energy spectrum of a partially restricted gapless semiconductor was investigated in the parabolic approximation. It was shown that 2D states should exist near the boundary even in the absence of an attractive electrostatic potential. These states are specific to gapless semiconductors of the HgTe type and become apparent only when the matrix structure of the Hamiltonian is taken into account. The dispersion law of such states is parabolic. When $k_y=0$, their energy coincides with the bottom of the conduction band, and their effective mass is greater than the mass of electrons in the bulk and takes on the value $m_s=4m_e/3$ in the limit $m_e/m_h \to 0$ (where m_h is the effective mass of a hole). However, as can be seen from Fig. 7, the 2D states that we observed have an effective mass $m_s \approx m_e$ at all values of the quasimomentum, making it impossible to interpret them as the interface states predicted in Ref. 6. This may be due to the special features of the model used in Ref. 6, viz., the zero boundary conditions and the parabolic approximation.

In the next section we examine the special features of the spectrum of 2D electrons in the surface quantum well of a gapless semiconductor with consideration of the nonparbolicity, i.e., accurately allowing for the interaction of the Γ_8 and Γ_6 bands.

4. CALCULATION OF THE ENERGY SPECTRUM OF ELECTRONS IN THE SURFACE QUANTUM WELL IN A GAPLESS SEMICONDUCTOR

The energy spectrum of the current carriers in heterostructures, such as single quantum wells and superlattices based on semiconductors described by a matrix Hamiltonian, including the Kane Hamiltonian, has been treated in various approximations. The Kane model, in which the terms containing the free-electron mass (m_0) and the interaction with distant bands are neglected, i.e., in which it is assumed that the mass of heavy holes (m_h) is infinite, as may be done in describing the spectrum of light particles, was used in the calculations in Refs. 7 and 8. Another widely employed approximation, in which the interaction with distant bands is taken into account, but the terms with m_0 are neglected, was described in detail in Refs. 21 and 22. The fewest approximations were made in Ref. 19, where Ram–Mohan, Yoo, and Aggarval accurately took into account the interaction of the Γ_8, Γ_6, and Γ_7 bands along with the interaction with distant bands with an accuracy to terms proportional to k^2, as well as the finite nature of the free-electron mass. The last factor greatly complicates the calculations and creates the appearance of higher accuracy. Inclusion of a term with m_0 in these problems is counterproductive from a physical standpoint, since it necessitates taking into account components of the wave function that are damped rapidly with increasing distance from the boundary, with a damping coefficient of the order of 10^{-8} cm, which is smaller than the lattice constant, i.e., the calculation unavoidably departs from the framework of the $\mathbf{k}\hat{\mathbf{p}}$ approach.

The spectrum of either symmetric heterostructures or boundary states at a single heterojunction was analyzed in all these studies. The experimental results presented above were obtained on somewhat different structures, viz., MIS structures. First, they are asymmetric structures. Second, when they are treated, a model of the semiconductor-insulator boundary must be selected, and, third, the behavior of the potential in the space-charge region must be specified.

The selection of the model of the semiconductor-insulator boundary is somewhat arbitrary, since our knowledge of a real semiconductor boundary and the electronic structure of an insulator is almost always very limited. If it is assumed that the main role in the boundary is not played by either electrons or holes from the semiconductor, the most acceptable model of a boundary would be the model proposed in Ref. 23, in which it was assumed that an insulator has the same energy structure as a semiconductor with the same momentum matrix element P and that the energies of the edges of the Γ_6 and Γ_8 bonds undergo jumps at the boundary (D_c and D_v, respectively), which are much larger than all the characteristic energies of the problem (Fig. 8).

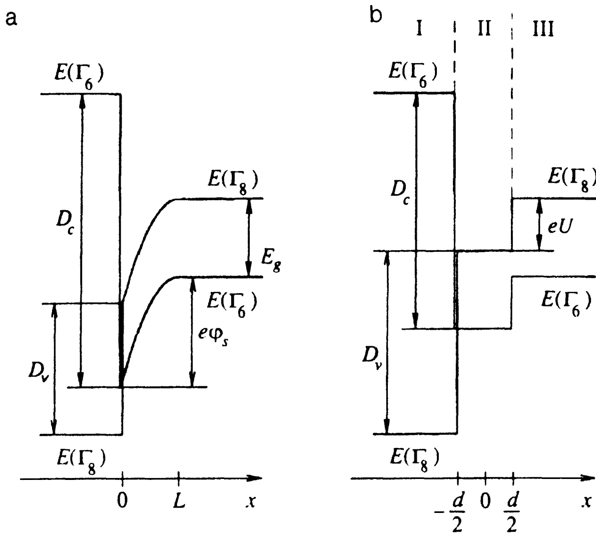

FIG. 8. Energy diagram of a gapless-semiconductor-insulator boundary in the presence of a smooth attractive potential (a) and a model rectangular potential (b).

The behavior of the potential in the space-charge region can be determined, as described above, from the Poisson equation, which is easily solved if the charge of the 2D electrons can be neglected. When the concentration of 2D electrons is high, their charge must be taken into account, i.e., the Schrödinger and Poisson equations must be solved simultaneously. The solution of the multiple-band Schrödinger equation for the structure shown in Fig. 8a is a complicated mathematical problem; therefore, for a qualitative analysis of the features of the electron spectrum in the surface quantum well of a gapless semiconductor we shall examine a model potential, i.e., a square well of depth $U=\varphi_s/2$ and width $d=L$ (Fig. 8b). The use of such a model potential instead of potential (5) in a quasiclassical calculation of the spectrum of 2D electrons gives similar results.

As in Ref. 7, we neglect the contribution of the Γ_7 spin–orbit split-off band, since the magnitude of the spin–orbit splitting in HgCdTe is of the order of 1 eV, which is much greater than the characteristic energies of the problem, and we assume that the heavy-hole mass is infinite. If, as above, the x axis is parallel to the direction of quantization (perpendicular to the plane of the structure) and the y axis is parallel to the two-dimensional wave vector in the plane of the surface of the semiconductor, the matrix of the Hamiltonian breaks up into two matrices corresponding to two "spin" states:

$$H_1=\begin{pmatrix} E(\Gamma_6) & (P/\sqrt{2})\,(i\hat{k}_x-\hat{k}_y) & (P/\sqrt{6})\,(i\hat{k}_x+\hat{k}_y) \\ (P/\sqrt{2})(-i\hat{k}_x-\hat{k}_y) & E(\Gamma_8) & 0 \\ (P/\sqrt{6})(-i\hat{k}_x+\hat{k}_y) & 0 & E(\Gamma_8) \end{pmatrix},$$

$$H_2=\begin{pmatrix} E(\Gamma_6) & (P/\sqrt{2})\,(i\hat{k}_x+\hat{k}_y) & (P/\sqrt{6})\,(i\hat{k}_x-\hat{k}_y) \\ (P/\sqrt{2})(-i\hat{k}_x+\hat{k}_y) & E(\Gamma_8) & 0 \\ (P/\sqrt{6})(-i\hat{k}_x-\hat{k}_y) & 0 & E(\Gamma_8) \end{pmatrix}, \quad (6)$$

(6)

where $\hat{k}_x=-i\,\partial/\partial_x$, $\hat{k}_y=-i\,\partial/\partial_y$, $E(\Gamma_6)$ and $E(\Gamma_8)$ are the energies of the Γ_6 and Γ_8 bands when $\mathbf{k}=0$, respectively.

If $E(\Gamma_6)$ and $E(\Gamma_8)$ do not depend on the coordinates, the general solution of the Schrödinger equation $H_i\Psi_i=E_i\Psi_i$ $(i=1,2)$ has the form[7]

$$\Psi_1=\begin{pmatrix} u_1 \\ v_1 \\ w_1 \end{pmatrix}=A\begin{pmatrix} (\sqrt{6}/P)\,[E-E(\Gamma_8)] \\ -\sqrt{3}(k_y+ik_x) \\ k_y-ik_x \end{pmatrix}\exp(ik_xx+ik_yy)$$
$$+B\begin{pmatrix} (P/\sqrt{6})\,[E-E(\Gamma_8)] \\ -\sqrt{3}(k_y-ik_x) \\ k_y-ik_x \end{pmatrix}\exp(-ik_xx-ik_yy). \quad (7)$$

The components of the wave vector k_x and k_y are related to the energy by the expression

$$k_x=\left(\frac{3[E-E(\Gamma_6)][E-E(\Gamma_8))}{2p^2}-k_y^2\right]^{1/2} \quad (8)$$

and Ψ_2 is distinguished from Ψ_1 by the replacement of k_y by $-k_y$.

The spectrum of 2D carriers in the structure depicted in Fig. 8b can be found by matching the wave functions of type (7) found for each of the regions at the boundaries. The matching conditions are easily obtained by intergrating the Schrödinger equation across each boundary. With the Hamiltonian that we have chosen, they reduce to con-

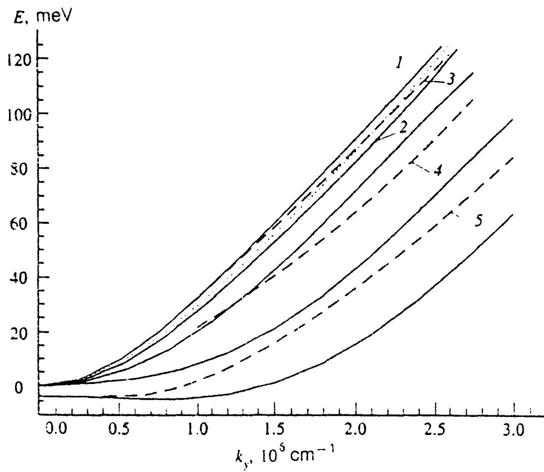

FIG. 9. Calculated dispersion laws for bulk states (curve *1*) and two-dimensional states (remaining curves). Curve *2*—$eU=20$ meV; curve *3*—$eU=40$ meV; curve *4*—$eU=80$ meV; curve *5*—$eU=120$ meV. The dotted curve is the dispersion law of the boundary states, i.e., $eU=0$. The solid curves correspond to the states with the wave function Ψ_1, and the dashed curves to the states with Ψ_2. $d=10^{-6}$ cm.

tinuity of the wave-function component u_i and the combination $\sqrt{3}v_i+w_i$ at the boundary.[7]

To find the spectrum of states localized at the boundary, we must leave only the solutions which decay at $x\to-\infty$ and $x\to\infty$ in regions I and III, respectively. Requiring fulfillment of the boundary conditions gives the secular equation

$$\begin{vmatrix} (E+eU)X_{\rm II}^- & (E+eU)X_{\rm II}^+ & 0 & -(E+eU+D_v)X_{\rm I} \\ (k_y+2ik_x)X_{\rm II}^- & (k_y-2ik_x)X_{\rm II}^+ & 0 & (k_y+2\kappa_{\rm I})X_{\rm I} \\ (E+eU)X_{\rm II}^+ & (E+eU)X_{\rm II}^- & -EX_{\rm III} & 0 \\ (k_y+2ik_x)X_{\rm II}^+ & (k_y-2ik_x)X_{\rm II}^- & -(k_y-2\kappa_{\rm III})X_{\rm III} & 0 \end{vmatrix}=0, \qquad (9)$$

where

$$X_{\rm I}=\exp\left(-\kappa_{\rm I}\frac{d}{2}\right),\quad X_{\rm II}^+=\exp\left(ik_x\frac{d}{2}\right),$$

$$X_{\rm II}^-=\exp\left(-ik_x\frac{d}{2}\right),\quad X_{\rm III}=\exp\left(-\kappa_{\rm III}\frac{d}{2}\right).$$

Here the energy E is measured from the bottom of the conduction band in the bulk of the semiconductor (region III); k_x is the component of the quasimomentum in region II; $\kappa_{\rm I}$ and $\kappa_{\rm III}$ are the decay decrements $[\kappa_{\rm I,III}=(ik_x)_{\rm I,III}]$ in regions I and III, respectively.

Equation (9) gives the dispersion law of the localized states corresponding to the wave function Ψ_1. The spectrum of states corresponding to Ψ_2 can be obtained by replacing k_y by $-k_y$ in (9). This equation was solved numerically for $E_g=-100$ meV, $P=8\cdot10^{-8}$ eV·cm, $D_c=1$ eV, and $D_v=2$ eV.

Further insight into the main features of the spectrum of 2D electrons in such a structure can be gained by examining the dispersion law of electrons $E(k_y)$ when the well has different depths and a fixed value of d (Fig. 9). It can be seen that in the absence of a well, i.e., when $U=0$, there should be a branch of boundary states (dotted line) whose energy at $k_y=0$ coincides with the bottom of the conduction band in the bulk solid. The special features of the behavior of this branch were discussed in detail in Ref. 24; the very same boundary states were investigated in the parabolic approximation in Ref. 6. As we mentioned above, in this approximation the dispersion law of the boundary states in the limit $m_e/m_h\to0$ is also parabolic and is described by an effective mass $m_s=4m_e/3$. It can be seen from Fig. 10 that consideration of the nonparabolicity causes the effective mass of the 2D states to be greater than the effective mass in the bulk only at small k_y, so that the dispersion laws of the boundary and bulk electrons remain similar at all k_y (Fig. 9). As the depth of the well increases, the effective mass at small k_y increases, but at large k_y the effective mass of the 2D states continues to remain close to the mass of the bulk states (Fig. 10). The nonmonotonic character of the plots of $m_s(k_y)$ at small k_y, at which the energy of the states is close to the degeneracy point in the bulk can be attributed to the form of the model potential, i.e., the abrupt step at the boundary between regions II and III. These qualitative features are relatively insensitive to the values of D_v and D_c and the ratio between them (as long as D_v, $D_c\gg E_g$ and $D_v>D_c$). One characteristic feature of 2D states in an asymmetric structure is the considerable difference between the energies of the states with wave functions Ψ_1 and Ψ_2, which correspond to different "spins" (Figs. 9 and 11). When the well is absent or its depth is small, only the "spin" state corresponding to Ψ_1 exists (Fig. 11). As the depth of the well is increased, the other "spin" state appears at a certain value of eU, which depends on k_y ($eU\approx35$ meV when $k_y=10^6$ cm^{-1}), and at large values of eU both states already exist at $k_y=0$ (Fig. 9). When the depth of the well is increased further, these states change places. This should correspond to reversal of

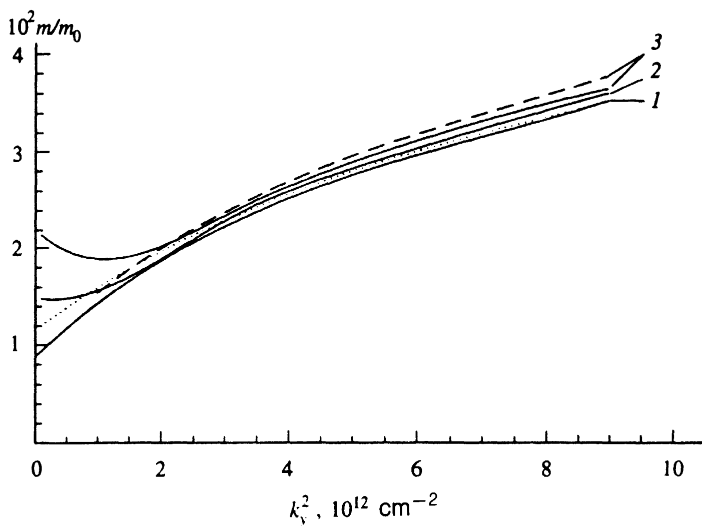

FIG. 10. Dependence of the effective mass on k^2 for bulk states (curve *1*), for 2D states when $eU=20$ meV (curve *2*), for 2D states when $eU=40$ meV and $d=10^{-6}$ cm (curve *3*), and for $eU=0$ meV (curve *4*). The solid curves correspond to the states with the wave function Ψ_1, the dashed curve corresponds to the states with Ψ_2, and the dotted curve corresponds to the boundary states.

the sign of the g factor, and at large values of eU their energies become close to the quasiclassical values (Fig. 11).

5. COMPARISON WITH EXPERIMENTAL RESULTS

Before proceeding to an analysis of the experimental results in the context of the present model, we wish to make several comments:

1. The theoretical calculation was performed for a model (rectangular) potential, rather than the real potential in the surface region of a semiconductor.

2. The model of the insulator contains two additional parameters D_c and D_v, which contribute to specifying the quantitative characteristics of the 2D electrons (but not the qualitative features of their spectrum).

3. The calculation was performed without consideration of the interaction with the Γ_7 spin–orbit split-off band, which is significant in a quantitative treatment of the experimental results.

Therefore, in comparing such an idealized calculation with experimental data, it would be more judicious to compare relative parameters of the spectra of the two-dimensional and bulk states (for example, the ratio m_s/m_e at a single value of k_y), and no special significance should be attached to quantitative agreement between absolute values.

The surface potential needed to form 2D states with an experimentally observed binding energy E_i, which is defined as the difference between the energies of the bulk and two-dimensional states at a given k_y (Fig. 3), can be evaluated in the context of the model considered in the pre-

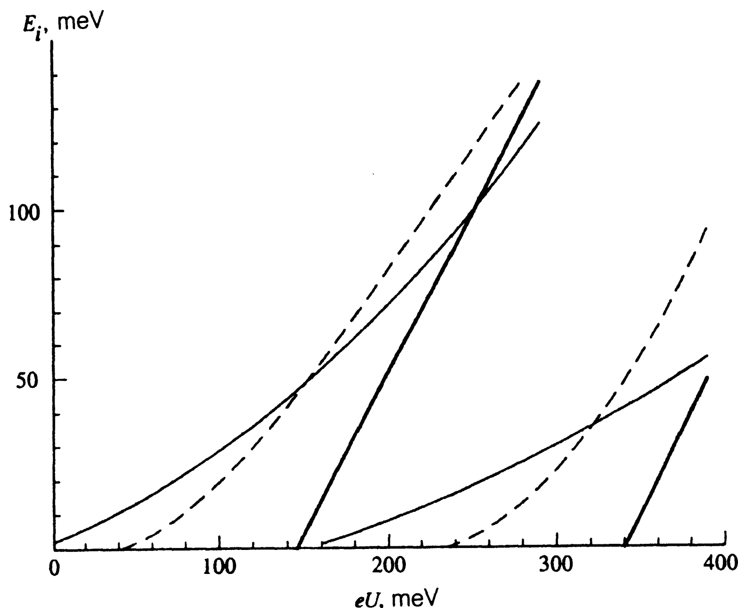

FIG. 11. Dependence of the binding energy E_i at $k_y=10^6$ cm^{-1} on the depth of the well when $d=10^{-6}$ cm. The solid curves correspond to the states with the wave function Ψ_1, the dashed curve corresponds to the states with Ψ_2, and the thick solid curve corresponds to the quasiclassical calculation.

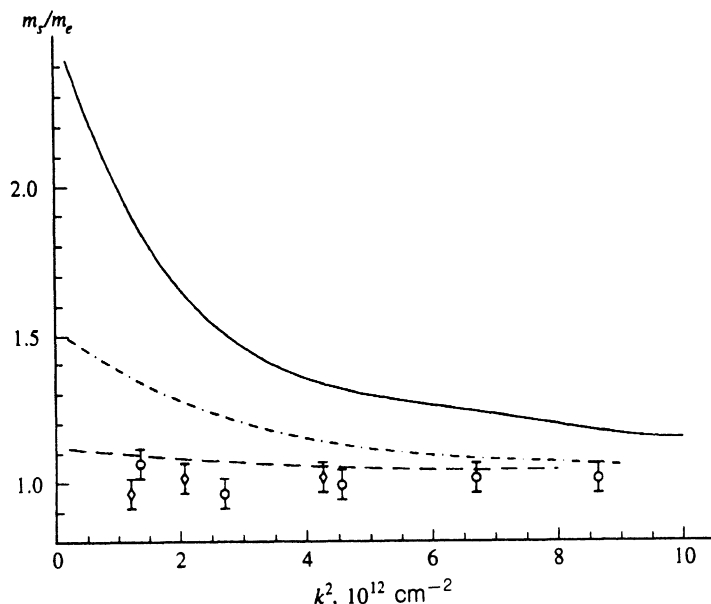

FIG. 12. Ratio of the effective mass of 2D electrons to the effective mass in the bulk solid with the same k_y. Points—experimental data for junctions from the first (○) and second (◇) groups; solid curve—quasiclassical calculation; dash-dot and dashed curves—results of calculations for 2D states with junctions from the first and second groups, respectively.

ceding section. For a tunnel junction from the first group, whose results are presented in Fig. 3, this gives $eU \approx 70$ meV when $V \sim 30$ mV and $eU \approx 40$ meV when $V \approx 140$ mV. Thus, the depth of the potential well needed to ensure a given E_i is significantly smaller than the depth in the quasiclassical model, and the change in its value upon application of a voltage amounts to only 1/4 of the voltage applied to the tunnel junction.

The experimental results obtained on tunnel junctions from the second group, in which an angular dependence of the position of the oscillation maxima typical of 2D states is observed, despite the equality between the periods of the oscillations in both orientations of the magnetic field to within the experimental errors, can also be understood in the context of the model considered. In these junctions there is essentially no potential attracting the electrons, and the tunneling conductivity oscillations observed when $\mathbf{H} \| \mathbf{n}$ are attributed to tunneling into boundary 2D states. As can be seen from Fig. 9, the binding energies for these states should amount to only 1–3 meV over the entire range of k_y. The other most significant inconsistency between the quasiclassical model and experiment is the disparity between the values of the effective mass of the 2D states. The quantum-mechanical calculation described above, which takes into account the multicomponent nature of the wave function and the nonparabolicity of the spectrum, shows that the effective mass of the 2D carriers is, in fact, close to the mass in the bulk of the semiconductor in the experimentally accessible range $k_y > 10^6$ cm^{-1} (Fig. 12).

Now the lack of spin splitting upon tunneling into two-dimensional states (Figs. 1 and 5) can be understood. As can be seen from Figs. 9 and 11, when the depth of the well is small, there is only one "spin" state localized in it. As calculations with parameters corresponding to the junctions from the first and second groups show, just such a situation is realized when $V > 20$–60 mV. When the well is deeper, spin splitting should be observed, and we hope that further investigations of tunneling will make it possible to study it experimentally and to compare the experimental results with calculations in detail. There may be an impression that 2D electron states always form on the boundary of a gapless semiconductor, and then our claim in Ref. 14 that we observed tunneling into bulk states in both orientations of the magnetic field no longer seems reasonable. Actually, calculations employing the model described above show that even a small electron-repelling potential (2–5 mV) results in the disappearance of boundary 2D states.

6. CONCLUSIONS

The use of tunneling spectroscopy in a quantizing magnetic field thus makes it possible to investigate two-dimensional electron states localized at the boundary of a gapless semiconductor. It has been shown that size quantization of electrons occurs in a substantially different manner in a gapless semiconductor than in semiconductors in which the conduction band is the Γ_6 band. The overall picture may be described in the following manner. Electrons in a gapless semiconductor are effectively attracted to the boundary even in the absence of an electrostatic potential. This attraction depends on the "spin" and k_y, so that in one of the two "spin" states it is sufficient for the formation of a 2D state localized at the boundary. In a gapless semiconductor with a small value of $|E_g|$, the spectrum of such boundary states $[E(k_y)$ and $m_s(k_y)]$ is very similar to the spectrum of bulk states except in a small range of k_y near zero.

When there is an electron-attracting potential on a gapless-semiconductor-insulator boundary, the binding energy of the 2D states increases at $k_y > 1/d$, but the effective mass remains close to the bulk value at these values of k_y. When the potential is increased, the total attraction be-

comes sufficient for localization of the other "spin" state, and as the electrostatic attraction is increased further, the parameters of the 2D states approach those calculated in the quasiclassical model.

A small repulsive potential near the surface of a gapless semiconductor is sufficient for the disappearance of boundary 2D states.

We express our thanks to V. V. Kruzhaev for his continual interest and concern with this work, and G. I. Kharus and N. G. Shelushinina for their fruitful discussions.

This work was supported, in part, by a Soros Foundation Grant awarded by the American Physical Society. It was also partially supported by a grant from the State Committee of the Russian Federation on Scientific Affairs and Higher Education.

[1)]Detailed investigations of the angular dependence reveal that the additional maxima which were observed for several samples at high applied voltages in strong magnetic fields (for example, the maximum at $H=4$ T in Fig. 5) and might have been attributed to spin splitting are caused by tunneling into Landau levels of bulk states.

[2)]"One-spin" states can exist in gapless semiconductors. For example, the additional branch of boundary states predicted in Ref. 6 is one-spin.

[1]T. Ando, A. B. Fowler, and F. Stern, "Electronic properties of two-dimensional systems," Rev. Mod. Phys. **54**, 437–672 (1982).
[2]U. Ekenberg, Phys. Rev. B **40**, 7714 (1989).
[3]T. Ando, J. Phys. Soc. Jpn. **51**, 3893 (1982).
[4]V. F. Radantsev, Fiz. Tekh. Poluprovodn. **22**, 1796 (1988) [Sov. Phys. Semicond. **22**, 1136 (1988)].
[5]V. F. Radantsev, T. I. Deryabina, L. P. Zverev *et al.*, Zh. Eksp. Teor. Fiz. **88**, 2088 (1985) [Sov. Phys. JETP **61**, 1234 (1985)].
[6]M. I. D'yakonov and A. V. Khaetskiĭ, JETP Lett. **33**, 110 (1981).
[7]M. V. Kisin and V. I. Petrosyan, Fiz. Tekh. Pouprovodn. **22**, 829 (1988) [Sov. Phys. Semicond. **22**, 523 (1988)].
[8]R. A. Suris, Fiz. Teor. Poluprovodn. **20**, 2008 (1986).
[9]D. C. Tsui, Phys. Rev. B **8**, 2657 (1973).
[10]L. P. Zverev, V. V. Kruzhaev, G. M. Min'kov, and O. É. Rut, Zh. Eksp. Teor. Fiz. **80**, 1163 (1981) [Sov. Phys. JETP **53**, 595 (1981)].
[11]L. P. Zverev, V. V. Kruzhaev, G. M. Min'kov *et al.*, Fiz. Tverd. Tela **26**, 2943 (1984) [Sov. Phys. Semicond. **26**, 1778 (1984)].
[12]O. É. Rut, V. V. Kruzhaev, and G. M. Min'kov, Fiz. Tverd. Tela **23**, 3212 (1981) [Sov. Phys. Semicond. **23**, 1869 (1981)].
[13]I. V. Gavriklyuk, Z. I. Kazantseva, N. V. Lavrik *et al.*, Poverkhnost' No. 11, 93 (1991).
[14]A. V. Germanenko, V. V. Kruzhaev, G. M. Minkov *et al.*, Semicond. Sci. Technol. **8**, 383 (1993).
[15]F. J. Ohkawa and Y. Uemura, J. Phys. Soc. Jpn. **37**, 1325 (1974).
[16]W. Zawadzki, J. Phys. C **16**, 229 (1983).
[17]L. P. Zverev, V. V. Kruzhaev, G. M. Min'kov, and O. É. Rut, JETP Lett. **31**, 154 (1980).
[18]W. Kraak, J. Kaldasch, P. Gille, T. Schurig, and R. Herrmann, Phys. Status Solidi B **161**, 613 (1990).
[19]L. R. Ram-Mohan, K. H. Yoo, and R. L. Aggarval, Phys. Rev. B **38**, 6151 (1988).
[20]J. R. Meyer, C. A. Hoffman, and F. J. Bartoli, Semicond. Sci. Technol. **5**, S90 (1990).
[21]L. G. Gerchikov and A. V. Subashiev, Phys. Status Solidi B **160**, 443 (1990).
[22]M. Altarelli, Physica B and C (Utrecht) **117/118**, 747 (1983).
[23]P. Sobkowicz, Semicond. Sci. Technol. **5**, 183 (1990).
[24]M. V. Kisin, Phys. Tekh. Poluprovodn. **24**, 1983 (1990).

Translated by P. Shelnitz